Design of a test facility for evaluating liquid hydrogen fuel level probes

S.O. Abi-Saad, J.W. Leachman

HYdrogen Properties for Energy Research (HYPER) Laboratory, School of Mechanical and Materials Engineering, Washington State University, Pullman, WA 99164-2920 USA

Email: jacob.leachman@wsu.edu

Abstract. Advances in liquid hydrogen vehicular fuel emphasize the need for continuous and reliable fuel gauging systems in dynamic environments. More specifically, there is a need for reliable comparisons and verifications of various fuel-level measurement systems. To address this need, an existing 250 L liquid hydrogen (LH2) dewar was retrofitted for simultaneous comparisons between modular liquid-level probes. A Gifford-McMahon (GM) cryocooler mounted on the custom dewar neck allows for variation of subcooling and management of ullage conditions within the dewar under static conditions. To simulate dynamic slosh conditions, a servomotor will be utilized to oscillate the dewar at a frequency conducive to sloshing. This paper describes the integrated design of the facility, including theoretical performance estimates of cool down and LH2 transfers to ensure compliance with the initial design specification in advance of system construction and commissioning.

1. Introduction

Liquid hydrogen is a powerful and sustainable fuel with the potential to propel humanity into space while also serving as an effective energy storage medium. These are just a few of the many reasons why liquid hydrogen is rapidly gaining traction as a fuel for aviation [1]. Fuel level measurements are paramount in providing an accurate usable fuel mass for aircraft propulsion systems. Traditionally, this usable mass can be calculated from the liquid level height and physical parameters such as temperature and pressure. However, the aviation industry demands durable, long-life measurement devices capable of precise mass determination, integrating multiple liquid level gauging methods for redundancy and compliance with FAA 25.1309 [20].

Liquid level sensors generally fall into two categories: point-level sensors and continuous-level sensors [2]. Point-level sensors typically consist of an array (or "rake") of sensing points that indicate discrete interface locations through a binary (on/off) output. Point-level sensors work well in defined static conditions and are easy to implement. However, point-level sensors often face challenges in dynamic environments (i.e, during fueling or sloshing), which can compromise the accuracy of level measurements [3]. In contrast, continuous-level sensors provide real-time sampling along the entire fluid column, offering a more detailed view of the fluid interface [1]. Although several continuous-level sensing technologies have been developed and tested

individually to demonstrate proof of concept and feasibility, no cross-comparison under identical operational conditions have been completed for side-by-side technology comparisons.

This paper identifies LH2 continuous level sensing technologies, examines limitations and integration challenges, and designs a test facility capable of simultaneously evaluating continuous liquid level probes under varied conditions (i.e., different liquid levels, fill conditions, ullage stratification, and dynamic sloshing). Thermally homogenous conditions present a challenge liquid-level measurement by eliminating temperature gradients and preventing stratification. The various continuous sensing devices will be compared against a point-level temperature rake for calibration and validation under different ullage, pressure, and sloshing conditions.

2. Literature Review.

There are several emerging techniques for continuous liquid hydrogen (LH2) level measurement, including radio-frequency, high-temperature superconducting sensors, capacitance, fiber optic sensors, and acoustic devices [2]. Each technology requires a unique method for integration, calibration, and mitigation of interference, as well as specific considerations for electrical pass-throughs. The primary emphasis of this literature review and Table 1 is the testing facilities, fluids, and conditions in which these level sensors have been tested.

Dodge et al. [1] surveyed the LH2 liquid-level sensors used in rockets. Historically, cylindrical capacitance probes have been the most common form of liquid level measurement throughout the history of NASA's LH2 use. These devices operate by applying an electrical field between two concentric coaxial cables to provide continuous propellant level indications based on the liquid's electric permittivity (a.k.a. the dielectric constant) [6]. However, these probes are sensitive to errors from motion and temperature variations [4]. Recently, this capacitive method has been extended to Electrical-Capacitive Tomography (ECT). ECT utilizes multiple electrodes around the tank perimeter to reconstruct the liquid distribution based on variations in electric permittivity. ECT provides detailed spatial reconstruction but requires complex calibration requirements and is sensitive to internal conductive obstructions that can distort measurements if unshielded [11]. However, strategically integrating conductive elements as electrodes can improve volumetric resolution.

Radio-frequency mass gauging (RFMG) operates by measuring the natural electromagnetic than eigenmode frequencies of a tank and comparing these frequencies with a database of RF simulations of the tank containing various fluid fill levels and liquid configurations [7]. RF sensors offer high sensitivity and full-tank measurements but are highly dependent on tank geometry and require conductive tank walls, which are vulnerable to electromagnetic interference (EMI) [9]. Zimmerli et al. [8] have shown significant sensitivity of RF sensors to tank material and geometry, emphasizing these constraints.

Superconducting MgB_2 wires have been implemented in several liquid hydrogen systems [13],[14]. These sensors measure the liquid level by leveraging the superconducting-to-normal state transition to achieve high sensitivity with minimal thermal impact. These sensors employ an external heating wire that exploits the distinct thermal responses of wetted versus unwetted sections, enabling level detection even under thermally homogeneous tank conditions. The transition temperature of MgB_2 is T_c= 39 K [14], these sensors have been tested under a variety of conditions, including within optical cryostats, under dynamic sloshing, and in both aluminum and stainless-steel tanks. The primary challenge for MgB_2 sensors is environmental magnetic interference. However, when operated under controlled magnetic conditions, these sensors offer stable performance and reliable calibration [14].

Fiber optic sensors, particularly Fiber Bragg Grating (FBG) sensors, measure liquid levels through strain-induced wavelength shifts in optical fibers. Changes in liquid level cause mechanical strain or thermal deformation in the fiber, altering the reflected Bragg wavelength [15]. FBG sensors offer high sensitivity, resolution, and electromagnetic interference immunity,

making them ideal for cryogenic aviation applications, though rigorous dual-phase calibration is required to ensure accuracy under varying cryogenic temperatures [17]. Similar to the MgB_2 sensor, the fiber optic strain gauge method also utilizes a heating wire which is beneficial in thermally homogeneous conditions.

A final and classic category of liquid level measurement is the pressure-volume-temperature (PVT) method, which relies on differential pressure measurements and/or floats utilizing buoyancy in the liquid. PVT methods are more suitable for static environments with well-defined ullage space temperatures [5]. As these methods are non-ideal for sloshing and dynamic conditions, there remains a need to develop more reliable and continuous forms of liquid level sensing.

Table 1: Continuous liquid level probe literature survey including the experimental apparatus and/or modelling emphasis, experimental conditions, and locations of the liquid level devices.

Source	Method	Cryogen	Tank Conditions
Edwards et al. [6]	Capacitance	LN2 LH2	Pressurized conditions (0.3 - 2.7 bar) in cryostat tested a coaxial capacitance probe with reference rake of silicon diode temperature sensors space 0.76 cm.
Lockhart et al. [7]	RF	LOX LH2	Aluminium tank 61 cm in diameter, 61 cm in height with one set of four resistance temperature probes at discrete levels.
Zimmerli et al. [8]	RF	LOX	Aluminium 46.1 L right cylinder tank with 61 cm diameter & utilized a rigid coax cable as the RF antenna with scale reference.
Wilson et al. [9]	RF	LH2	Modeled different mounting configurations, optimal height ratio of 7/16 from top-center mounted flange.
Zimmerli et al. [10]	RF	LOX	Tanks constructed from carbon fiber composite & metal parts within the tank, benchmarking as a reference for tank fill.
Storey et al. [11]	ECT	NOVEC	ECT system is outfitted to a 3 m spherical tank with 16 electrodes insulated by polymer composite from aluminium walls. Included internal obstructions and compared to a scaled measurement.
Behruzi et al. [12]	ECT	LH2	Six rings (tested both carbon fiber & aluminium) of 8 capacitance electrodes mounted inside a cylinder in LH2 cryostat.
Haberstroh et al. [13]	MgB_2	LH2	MgB2 in LH2 tested in a 100-500 mA with cross sectional area of 300 μm tested in range of pressures (1-5 bar).
Maekawa et al. [14]	MgB_2	LH2	Dynamic conditions with external heating MgB2 (6-9 W) tested in a 20 L aluminum optical cryostat as reference.
Sharma et al. [15]	Fiber optics	LN2	Tested at 3 bar. Calibrations were done by optical power to the sensors, 400Hz laser compared to mechanical pressure gauges.
Figueroa et al. [16]	FBG	LOX	Two sets of fiber optic strain gauges (FOSG) were tested in a dewar and compared to a differential pressure sensor.
Umesh et al. [17]	FBG	LN2	Two FOSG (1530 nm) bonded over resistance heating rod 20 cm apart in a cylindrical SS tank of diameter 25 mm and 1.2 m tall

This literature survey highlights the need for a unified, modular test facility designed to evaluate these sensor technologies simultaneously under identical, realistic cryogenic conditions, incorporating dynamic factors such as sloshing and fill conditions.

3. Preliminary Design.

The primary design constraints for the test facility include the retrofit of a 250 L liquid hydrogen dewar and integrating multiple liquid level devices that can operate between 3–5 bar saturated conditions while ensuring isothermal ullage conditions within the dewar. Dynamic environments that cause sloshing can be achieved through a servomotor attached via a rotary arm to the dewar base. The physical constraints of the dewar included the 15.3 cm diameter dewar neck, which accommodates all probes, electronics, and heat exchanger. The dewar geometry is a 2:1 ellipsoid with an internal lining of SS304, 71.1 cm diameter, and 81.3 cm height. This dewar is maintained within a vacuum jacket at a pressure of about 2.2×10^{-4} Pa.

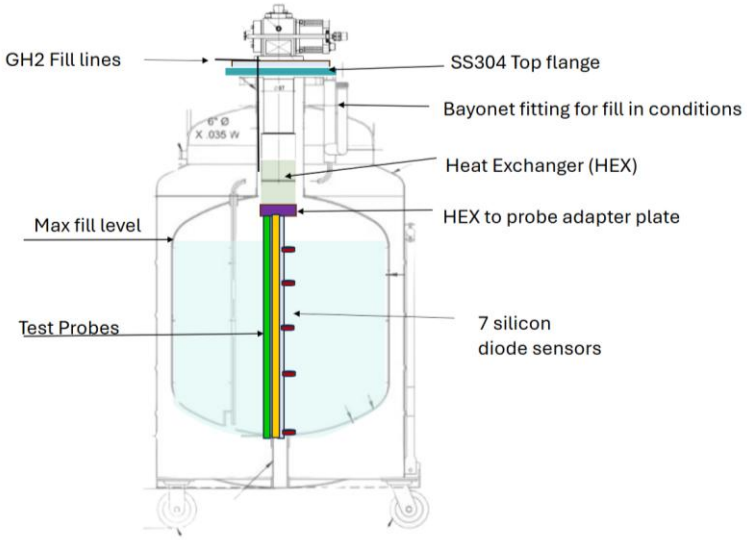

Figure 1: Conceptual design and layout of the liquid level test facility. The Sumitomo RDK500B2 will sit on top of a SS316 flange that will have all the necessary electronic pass-throughs.

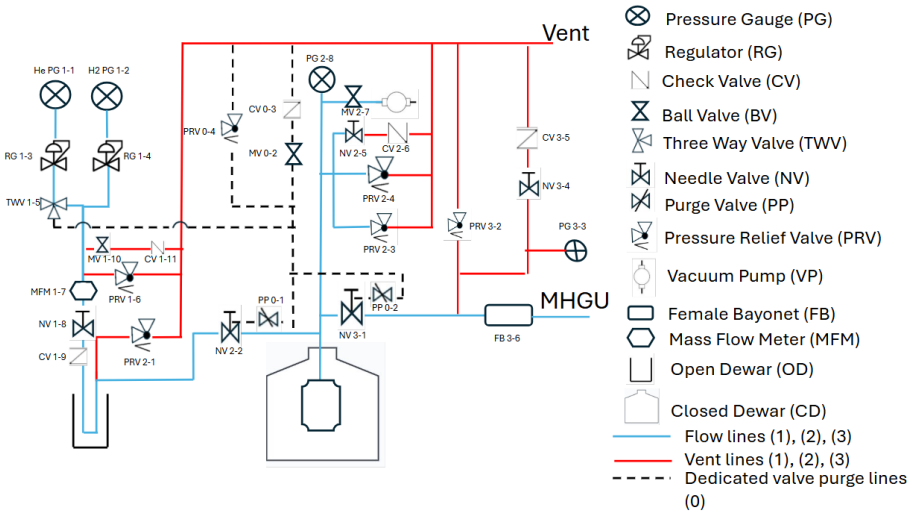

Figure 2: Piping and instrumentation diagram (P&ID) for the liquid level test facility. Interfaces with Mobile Hydrogen Generation Unit (MHGU) [19] a pre-existing capability at HYPER for in-situ liquification in a 60 L ~ roughly 3.4 kg of liquid hydrogen dewar with a two-stage GM cryocooler with 20 W at 20 K.

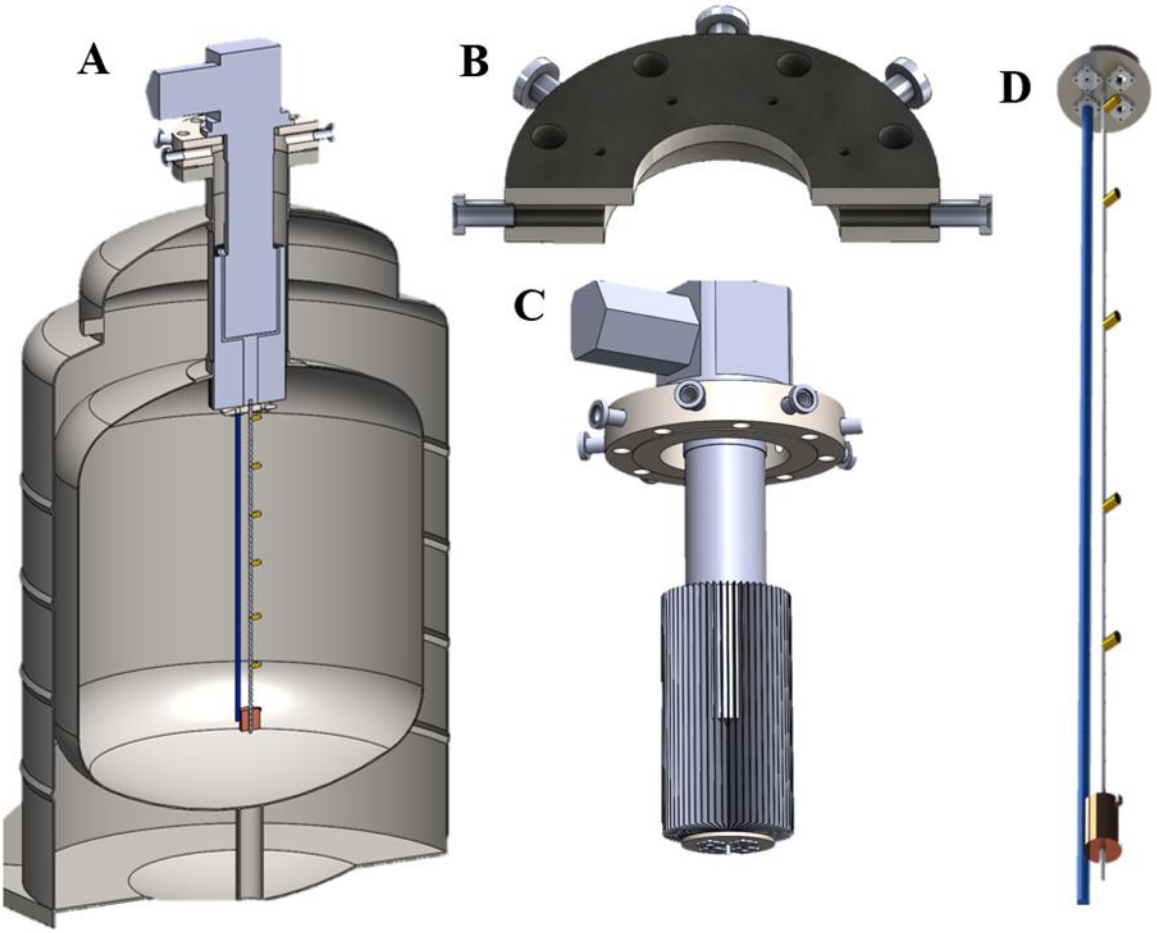

Figure 3: Preliminary design of the liquid-level test facility: (Panel A) the complete assembly; (Panel B) the top plate with hermetic electronic pass-throughs via VCR fittings; at bottom center (Panel C) the probe holder and finned heat exchanger mounted on a central SS316 rod that supports the reference rake; and Panel C shows the probe adapter (Panel D) and reference rake carrying diode sensors distributed throughout the ullage space.

Liquefaction within the dewar will be managed by a liquid nitrogen (LN2) precooler, Sumitomo RDK 500B2 GM Cryocooler, and a finned heat exchanger. The precooler will enter through an open LN2 dewar through a coiled heat exchanger and enter through the GH2 fill lines in Figure 1. These lines will enter through the dewar neck and through the finned heat exchanged shown in Figure 2 that will further be cooled by the single-stage cryocooler that pulls 50 W at 20 K. The heat exchanger differs from prior designs due to the single-stage nature of the cryocooler. Directly beneath this heat exchanger a liquid level probe adapter will be installed to test the developing probes, as shown in Figure 3C. A vibrational dampening material will be installed between the probe holder and cryocooler to mitigate vibrational effects on the liquid level sensor readout.

The holder will incorporate a central stainless-steel 316 tube featuring tapered holes spaced at 1 cm intervals as shown in Figure 3D above. This design enables the positioning of reference sensors, enhancing testing capabilities based on different test plans, as illustrated in Figure 3. The probe holder will be designed with twenty open slots to accommodate interchangeable level-sensing probes as shown in figure 3C. Each probe will be mounted using custom brackets. A heater

installed at the base of the rod will enable precise control of the liquid level during testing and venting.

Radio-frequency (RF) sensors will be evaluated in a dedicated setup due to the dependence on a highly calibrated library of transverse magnetic (TM) resonant modes, which shift with changes in tank geometry and require a conductive enclosure to form a resonant cavity. Moreover, emitted electromagnetic resonances can interfere with other probes. In contrast, MgB_2 superconducting sensors and fiber-optic sensors will be tested simultaneously alongside electrical capacitance tomography (ECT) diodes. The stainless-steel 304 dewar shell serves to suppress unwanted electromagnetic interference (EMI) and stray signals, providing a controlled test environment for these non-RF probes. By contrast, radio-frequency mass-gauging (RFMG) benefits from the conductive dewar acting as a cavity to enhance TM mode resonances; accordingly, RF testing will be implemented in a separate, purpose-designed apparatus in future work.

4. Testing Capabilities and Conditions.

Testing a variety of conditions is critical in having a complete analysis of the accuracy of these probes for real-time implementation and use. For this reason, this test facility is designed to be capable of testing static, fill, venting, and sloshing conditions. The facility will interface with the pre-existing Mobile Hydrogen Generation Unit (MHGU) at Washington State University, which will enable safe LH_2 transfers [19]. Static fill levels are shown in Table 2 below and are limited to 120 L in guidance with NFPA LH2 capacity standards. The dewar installed on MHGU is from CLH manufacturing model series with a smaller 60 L capacity, two-stage GM cryocooler capable of 20 W cooling capacity at 20 K. User control over the ullage pressure of each dewar will allow for liquid transfers between dewars. This allows tests with different pressures, fill, and venting conditions. The pressure in the dewar's ullage will be monitored via a pressure transducer installed on the existing pressure gauge. Isothermal conditions will be achieved through the finned heat exchanger that extends into the dewar cavity.

Table 2: Testable fill levels within the 250 L dewar, liquefaction time was calculated with the ideal SEC. An additional 8 hours is the expected cooldown time of the gas in the dewar ullage. The maximum liquid capacity is 120 L due to site capacity limitations.

Volume Fill (L)	Fill height (cm)	Mass (kg)	Fill level (%)	Relative fill level (%)	Ideal liquefaction time (days)	LN2 Precool (days)
120	36.1	7.82	100%	48%	~ 21	~ 4
90	28.6	5.87	80%	36%	~ 17	~ 3
60	21.0	3.91	60%	19%	~ 13	~ 2
30	8.9	1.96	40%	12%	~ 9	~ 1
0	0	0	0	0	0	0

A transient numerical model of liquid hydrogen transfer through a 0.635 cm diameter vacuum-jacketed bayonet line between the MHGU supply dewar and the 250 L receiving dewar was developed (Figure 2). The transfer line segment analyzed with Eq. (1) is this bayonet connection. The model assumes saturated liquid conditions with no venting. At each timestep, it updates ullage pressure, temperature, density, volume, and internal energy in each dewar to calculate the mass flow rate until pressure equilibrium is reached. Flow is determined from an energy balance using the Darcy–Weisbach equation for major frictional losses [21] together with empirical loss coefficients for bends, entrances, and exits.

$$P_1 - P_2 = \sum\left(f_{D,i}\frac{L_i}{D_i}\rho\left(\frac{2\dot{m}}{\rho_i * A_c}\right)^2 * \frac{1}{2}\right) + \sum\frac{K_{loss,i}}{2g} * \left(\frac{2\dot{m}}{\rho * A_c}\right)^2 \quad (1)$$

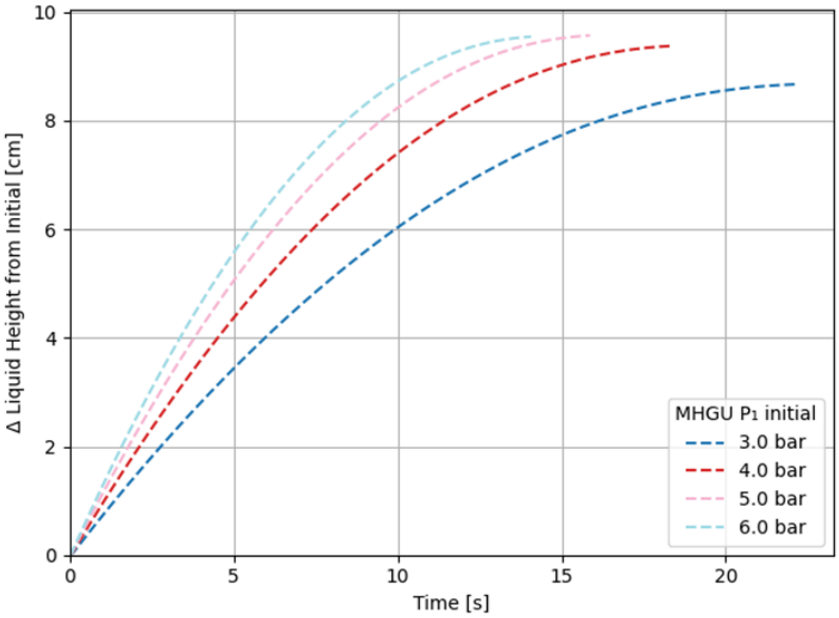

Figure 4: Change in liquid height (cm) versus time (s) due to mass transfer from the MHGU source into the 250 L receiving dewar at various driving pressures.

Here, P_1 is the driving pressure at the supply dewar, and P_2 is the pressure at the receiving dewar. The friction factor is calculated using the Colebrook–White correlations depending on the Reynolds number regime [21]. The temperature of the liquid and vapor phases is assumed to remain at saturation conditions corresponding to the instantaneous ullage pressure in each dewar.

The calculation model is transient and one-dimensional. Each dewar is represented by two thermodynamic control volumes (liquid and vapor). At each timestep, pressure differences between dewars drive flow, and ullage conditions are updated accordingly. A geometric algorithm converts liquid volume into fill height, accounting for the cylindrical midsection and semi-ellipsoidal end caps of the receiving tank (Figure 4).

The transfer continues until pressure equilibrium is reached between the dewars. While the model neglects two-phase effects, these simplifications contribute to its higher predicted flow rates under a geometric Darcy–Weisbach formulation Eq. (1). It assumes a pre-cooled line, which is achievable through procedural conditioning to minimize thermal resistance. It predicts faster-than-expected fill times, which aligns with observed results but still enables flow control through procedural steps such as venting and line pre-chilling. Despite these simplifying assumptions, the model and Figure 4 above capture system behavior and allow tuning for more accurate performance prediction. Under these conditions, continuous level probes can be quantitatively benchmarked against point-level rakes, with fill height determined from volume to support repeatable and representative sensor evaluation under transient LH_2 transfer scenarios.

5. Conclusions

A preliminary design for a modular liquid hydrogen level-gauging test facility enables direct comparison of emerging liquid hydrogen level sensing technologies. This facility will support simultaneous evaluation of MgB_2 superconducting probes, capacitance-based sensors, and fiber optics. Radio frequency mass gauging sensors will be evaluated in a separate setup to prevent

electromagnetic interference and to simplify the calibration of transverse magnetic (TM) modes. The facility can reproduce a range of conditions, including multiple fill levels, ullage pressures, dynamic filling, and controlled sloshing. The next design phase will focus on integrating the servo motor and configuring the dedicated radio frequency testing apparatus. This unified test facility serves as a new capability for comparing multiple sensor technologies under varied cryogenic conditions. Validating sensors in these regimes, we ensure that fuel-gauging technologies can reliably track liquid hydrogen mass in the different ullage pressures, temperature, and dynamic conditions for aviation service, thus supporting safe operations, regulatory compliance, and confidence in zero-emission propulsion systems.

Acknowledgement

These designs and results have been established in collaboration with Airbus.

References

[1] Dodge F 2008 *NTRS* CR-2008-215281
[2] Olsen W A 1962 Adv. Cryogenic Eng. 8 342–359
[3] Burgeson D, Petalozzi W, Richards R, 1964 *Adv. Cryog. Eng.* **10** 416–422
[4] Dresar N T 2004 *Cryogenics* **44** 515–523
[5] Dresar N T 2006 PVT *Cryogenics* **46** 118–125
[6] Edwards L and Haberbusch M 1993 *NTRS* NASA CR-109763
[7] Lockhart J 1966 *NTRS* NAS 8-11476
[8] Zimmerli G, Vaden K, Herlacher M, Buchanan D, and Dresar N 2007 *AIAA* **45** 1-19
[9] Wilson J, and Zimmerli G 2012 *NTRS* NASA TM-2012-217267
[10] Zimmerli G, Fischer D, Asipauskas M, Kory C, O'Connor A, and Rice A 2024 *AIAA* **2025 -0959**
[11] Storey J, Marsell B, Elmore M, and Clark S 2023 *NTRS* NASA/TP-20230012805
[12] Behruzi P, Hunt A, Foster-Turner R, Fischer A, 2023 *AIAA* **2023-1085**
[13] Haberstroh C and Zick G 2006 *AIP Conf. Proc.* **823** 679–684
[14] Maekawa K, Takaaki M, Hamaura T, Suzuki K, Matsuno Y, Fujikawa S, 2016 *IEEE Trans. Instrum. Meas.* **27-4**
[15] Sharma M 1979 NTRS NAS9-15454
[16] Figueroa F, Mitchell M, Langford L, 2004 *IMTC Instrument and Measurement Technology Conference*
[17] Umesh S , Rajan L 2021 *Second International Conference on Smart Technologies in Computing, Electrical and Electronics (ICSTCEE)* pp 1–5
[18] Parker A and Richards L 2015 *Cryogenic liquid level sensor apparatus and method* U.S. Patent **9 074 921**
[19] Richardson I 2022 *IOP Conf. Ser.: Mater. Sci. Eng.* **1240** 012077
[20] Federal Aviation Administration. 2022. *14 CFR §25.1309 – Equipment, Systems, and Installations*. U.S. Department of Transportation.
[21] White F, *Fluid Mechanics*, 9th ed., McGraw-Hill, 2021.